Carbohydrate Polymers 104 (2014) 191–198

Contents lists available at ScienceDirect

Carbohydrate Polymers

journal homepage: www.elsevier.com/locate/carbpol

Enhancement of cell viability by fabrication of macroscopic 3D hydrogel scaffolds using an innovative cell-dispensing technique supplemented by preosteoblast-laden micro-beads

HyeongJin Lee[a,1], SeungHyun Ahn[a,1], Wook Chun[b], GeunHyung Kim[a,*]

[a] Department of Bio-Mechatronic Engineering, College of Biotechnology and Bioengineering, Sungkyunkwan University, Suwon, South Korea
[b] Department of Surgery, College of Medicine, Hallym University, Hangang Sacred Heart Hospital, Seoul, South Korea

ARTICLE INFO

Article history:
Received 28 August 2013
Received in revised form 6 January 2014
Accepted 8 January 2014
Available online 19 January 2014

Keywords:
Cell-laden beads
Alginate
Tissue regeneration
3D scaffold
Bone

ABSTRACT

We propose a new cell-encapsulated dispensing method consisting of hydrogel struts, embedded with cell-laden micro-beads. To develop the scaffolds, we accommodated a three-axis robot dispensing system and aerosol spraying of a cross-linking agent to effect tentative surface gelation of hydrogel alginate struts. To show the feasibility of the method, we used pre-osteoblast (MC3T3-E1) cells. Using this technique, we obtained a reasonable cell viability (>90% after several culture periods) relative to that of a scaffold onto which cells were dispensed in the conventional manner, and successfully fabricated a realistic macroscopic pore-size in a controlled manner with 100% pore-interconnected 3D alginate hydrogel scaffolds of 20 mm × 20 mm × 6 mm.

1. Introduction

Generally, cell-laden three dimensional (3D) structures have been fabricated using bottom-up techniques, such as cell-sheet engineering (Yamato & Okano, 2004), cell printing (Cohen, Malone, Lipson, & Bonassar, 2006; Cohen et al., 2011; Mironov, Kasyanov, & Markwald, 2011) and dispensing (Ahn, Lee, Bonassar, & Kim, 2012; Fedorovich et al., 2012), laser-assisted methods (Ovsianikov et al., 2010), and cell-agglomerating methods, using moulds of various shapes (Matsunaga, Morimoto, & Takeuchi, 2011) and spheroid microarrays (Fukuda & Nakazawa, 2005; Mironov et al., 2009). From the perspective of high cell-seeding efficiency and a homogeneous cell distribution, these methods are powerful tissue-regeneration tools (Mironov et al., 2009). Although these innovative technologies have various important advantages, some major issues remain. The problems are the fabrication of 3D cell-laden structure thicker than 300 μm with an appropriate pore structure (proper pore size, high porosity, and high degree of pore-interconnectivity) that facilitates transport of nutrients and exchange of metabolic waste (Pirlo, Wu, Liu, & Ringeisen, 2012; Gaetani et al., 2012) and keeping of high cell-viability in the middle region of printed cell blocks after finishing fabrication, because through the harsh processing conditions the cell-viability can be significantly decreased (Ahn, Lee, Bonassar, et al., 2012). However, to date it has been very difficult to directly print macro-sized cell-seeded alginate scaffolds with pore-controlled microstructure and simultaneously obtain high cell-viability of the porous structure.

In this study, a novel cell-dispensing process using a three-axis robot system, supplemented by aerosol cross-linking and cell-encapsulation using micro-sized beads resulted in high cell viability both at the surface and throughout the cross-sectional area of a large-scale microscopic structure (several millimetres). The use of micro-sized beads containing cells (MB-Cs) enhances cell viability in the dispensed 3D structure, which consists of alginate micro-sized struts capable of enduring the external shear/normal stresses during a micro-syringe process and protecting against the harmful effects of the cross-linking agent ($CaCl_2$). Our approach allows control over macro-scale shaping of a highly porous 3D structure consisting of micro-sized struts embedded with MB-C. Furthermore, the technique also enhanced cell viability both at the surface and throughout the cross-section compared to the method of cell dispensing without micro-beads. In this work, we used pre-osteoblast cells (MC3T3-El) to show the feasibility of this process during long culture periods by comparing a normal aerosol cell-dispensed alginate scaffold with one embedded with MB-Cs.

2. Experimental

Cell and materials: MC3T3-E1 (ATCC, USA) mouse calvaria osteoblast cells were cultured and maintained in α-minimum

* Corresponding author at: 2066 Sebu-Ro, Jangan-Gu, Suwon-Si, Gyeonggi-Do, South Korea. Tel.: +82 31 290 7828.
E-mail address: gkimbme@skku.edu (G. Kim).
[1] These authors contributed equally to this work.

0144-8617/$ – see front matter © 2014 Elsevier Ltd. All rights reserved.
http://dx.doi.org/10.1016/j.carbpol.2014.01.024

essential medium (Life Science, USA) containing 10% foetal bovine serum (FBS, Sigma–Aldrich, St. Louis, MO, USA). Low viscosity, high G-content nonmedical-grade LF10/60 alginate was obtained from FMC BioPolymers (Drammen, Norway) and $CaCl_2$ was from Sigma–Aldrich.

Preparation of cell and MB-Cs embedded alginate solution: Alginate hydrogels for dispensing were prepared using the technique and optimised processing conditions described previously (Cohen et al., 2006, 2011). The alginate was mixed with PBS to prepare 3.5 wt% alginate. In previous work, we used various weight fractions of alginate to fabricate 3D cell-laden alginate structure and the 3 ± 0.3 wt% is the most appropriate to fabricate 3D cell-laden structure (Ahn, Lee, Bonassar, et al., 2012). Before loading the cells and MB-Cs, the alginate solution was mixed with 0.5 wt% $CaCl_2$ at a 7:3 ratio to increase its viscosity. Cells and MB-Cs were mixed in the alginate solution using a three-way stopcock tool to a density of 1.2×10^5 mL^{-1}. The cell–alginate mix was loaded into a syringe barrel. To completely cross-link the cells embedded within the alginate scaffold, a second cross-linking procedure was conducted using a 2 wt% $CaCl_2$ solution in PBS.

Rheological measurements of cell- and MB-C-laden alginate solutions: A mixture of cells (1.2×10^5 mL^{-1}) and alginate solution (3.5 wt%) was subjected to assessment of rheological properties using a rheometer (AR-2000, TA Instruments, New Castle, DE) equipped with a cone and plate geometry (10-mm radius, 108-μm gap, cone angle 2°). For dynamic shear measurements, dynamic frequency sweeps were conducted by application of 5% strain within the linear viscoelastic region over a frequency range of 1–100 rad s^{-1}. All dynamic experiments were conducted at 27 °C.

Fabrication of single alginate strut and 3D alginate scaffolds: A computer-controlled three-axis robot system (DTR2-2210T, Dongbu Robot, Bucheon, South Korea) supplemented with a micro-syringe dispenser and an aerosol humidifier (Tess-7400; Paju, South Korea) was used to fabricate a single strut of alginate and multilayered alginate structures at the processing temperature, 25–28 °C. In the dispensing system, pneumatic pressures for pure cells and MB-Cs and the stand-off distance between the nozzle (inner size = 410 μm, outer size = 720 μm) and working stage were 50 kPa and 25 kPa and 350 μm, respectively. In the aerosol-spraying process, we fixed the rate of continuous $CaCl_2$-aerosol flow onto the dispensing stage at 0.9 ± 0.2 mL min^{-1}. To obtain macroscopic and porous hydrogel scaffolds, each alginate layer adhered to the previous one perpendicularly, forming a 0°/90° strut structure. After the multilayered alginate struts fabricated had been dispensed with the $CaCl_2$ solution (first cross-linking process), the alginate scaffolds were again cross-linked (second cross-linking process) with 2 wt% $CaCl_2$ solution for 1 min.

Cell viability measurements: Cell- and MB-C-laden structures (single strut and 3D scaffold), were exposed to 0.15 mM calcein AM and 2 mM ethidium homodimer-1 for 45 min in an incubator. The stained structures were observed under a microscope (TE2000-S; Nikon, Tokyo, Japan) equipped with an epifluorescence attachment and a SPOT RT digital camera (SPOT Imaging Solutions, Sterling Heights, MI, USA). To evaluate cell viability, we captured the images and processed the number of green and red spots using the ImageJ program (NIH, Bethesda, MD, USA). Five randomly chosen images for each sample were analysed for four disks, yielding 20 images per group. The viability of the alginate structures was then determined.

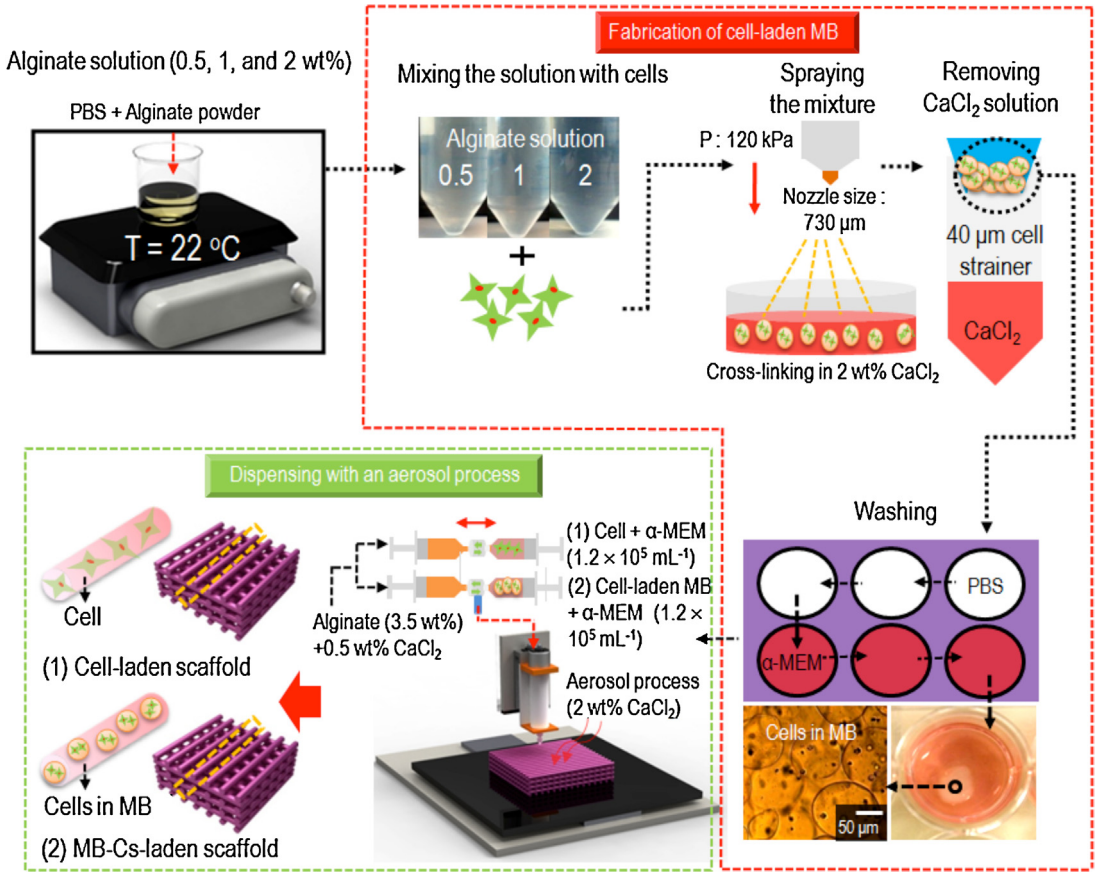

Fig. 1. Schematic of the fabrication of micro-bead (MB) and cell-laden 3D scaffolds using a three-axis robot system supplemented with an aerosol process. In this schematic, 'MB-Cs' indicates micro-beads containing cells.

The ratio of the number of live cells to the total number of cells (live and dead) was calculated using the software and the ratio was normalised to the initial cell viability, which was the value prior to cell–alginate extrusion. The initial viability was determined using trypan blue (Mediatech, Herndon, VA, USA).

In vitro cell culture: Cell-laden structures (micro-beads, single struts, and 3D scaffolds) were cultured and maintained in α-minimum essential medium containing 10% FBS and 1% antibiotics (antimycotic; Cellgro, Mediatech, Manassas, VA). The structures were incubated in an atmosphere of 5% CO_2 at 37 °C, and the medium was changed every second day.

Statistical analyses: Data are presented as means ± SD and were analysed for statistical significance by single-factor analysis of variance (ANOVA). The significance level was set at $^*p < 0.05$.

3. Results and discussion

3.1. Fabrication of cell-embedded micro-beads and scaffolds

Fig. 1 shows a schematic of the fabrication of the dispensed alginate struts containing cell-laden micro-beads. First, we mixed 0.5, 1, and 2 wt% alginate and cells at a density of 2.2×10^5 mL^{-1}. Second, the mixed solution was sprayed on $CaCl_2$ solution and micro-sized beads were produced (spraying conditions: pressure = 120 kPa, nozzle size = 730 μm). After cleaning several times with PBS and α-MEM solution, cell-embedded micro-beads were obtained. The MB-Cs (density = 1.2×10^5 mL^{-1}) were then re-mixed with an alginate solution (3.5 wt%) to fabricate a porous 3D structure consisting of layer-by-layer micro-struts. During dispensing of the solution, $CaCl_2$ solution aerosols (2 wt%) were fumed over the

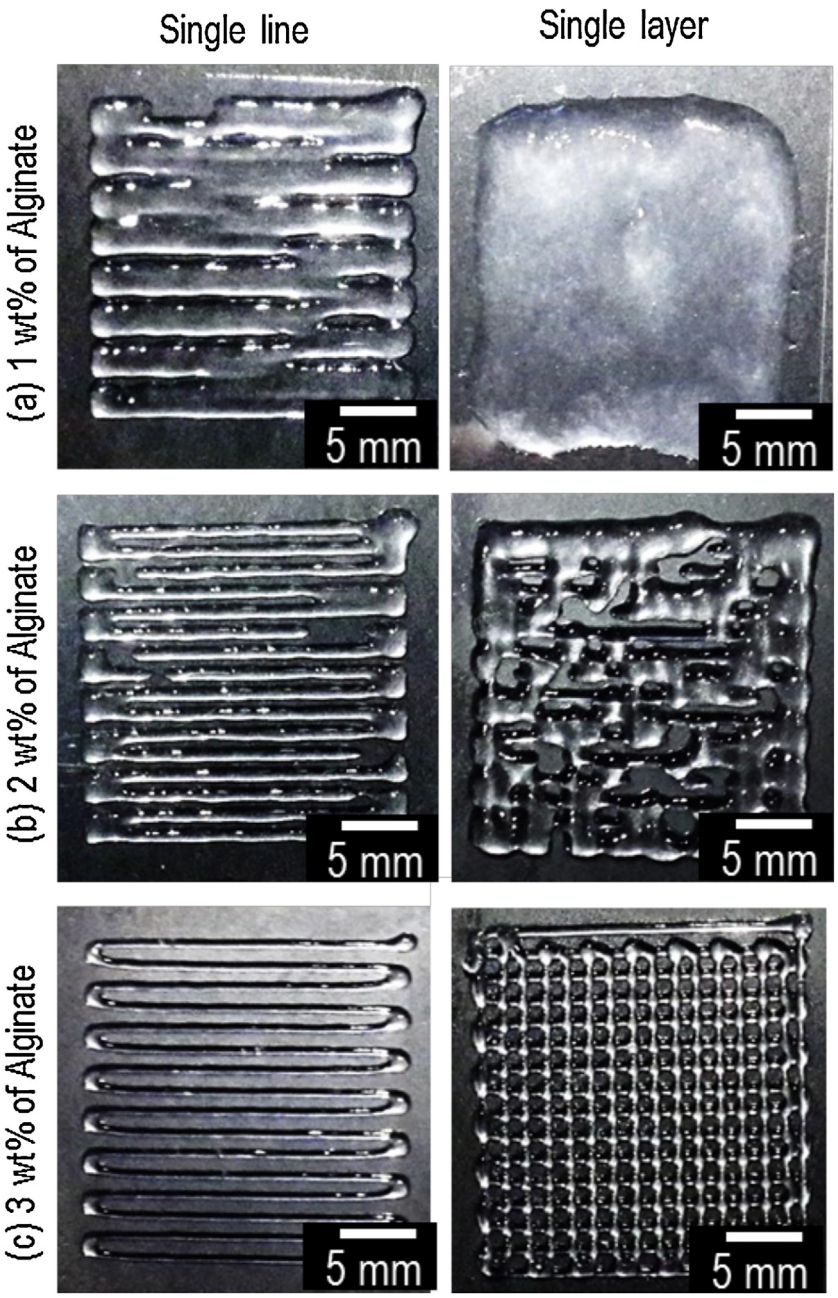

Fig. 2. Optical images (single line and single layer) of dispensed alginate solution for various weight fractions of alginate ((a) 1 wt%, (b) 2 wt%, and (c) 3 wt%) under the aerosol dispensing process.

alginate struts, resulting in tentative curing. We called this the first cross-linking process. Using this tentative aerosol process, the dispensed struts were not destroyed, resulting in maintenance of the designed pores of the 3D scaffold. After several layers of perpendicular alginate struts had been dispensed, the fabricated structure was re-cross-linked with calcium chloride solution (2 wt%) to stabilise the 3D pore structure and shape. When the weight fraction of calcium chloride solution was over 2 wt%, the cell-viability of the cross-liked cell-laden struts was rapidly decreased (Ahn, Lee, Bonassar, et al., 2012). We called this the second cross-linking process. After cleaning as before, two 3D hydrogel scaffolds were generated: (1) a cell-laden scaffold and (2) a MB-Cs-laden scaffold. The cell-laden alginate scaffold represented the control (Fig. 1). In this study, we set the weight fraction of alginate as a 3.5 wt% because the lower weight fractions (1 and 2 wt%) of the alginate cannot provide the structural stability during the aerosol dispensing process (Fig. 2(a)–(c)).

Several microfluidic methods, such as the internal gelation (Tan & Takeuchi, 2007), flow-focusing (Takeuchi, Garstecki, Weibel, & Whitesides, 2005) and T-junction (Okushima, Nisisako, Torii, & Higuchi, 2004) techniques, have been used to fabricate homogeneous and spherical micro-beads because non-spherical beads may result in reduced biocompatibility; even micro-beads with tails can cause fibrotic overgrowth of the surrounding tissue (Lum, Krestow, Tai, Vacek, & Sun, 1992; Park, Iwata, & Ikada, 1998). Of these, the internal gelation method results in fabrication of spherical beads of a uniform size distribution, with diameters of 94–112 μm (Tan & Takeuchi, 2007). However, to obtain a sufficient amount of cell-embedded micro-sized beads using a fast gelation process, development of a suitable mass production method was necessary. Therefore, we used a low-pressure spraying method.

To obtain optimised cell-embedded micro-beads, we used 0.5, 1, and 2 wt% alginate solutions with an identical cell density (Fig. 3(a)–(c)). Cells were well-embedded in the alginate

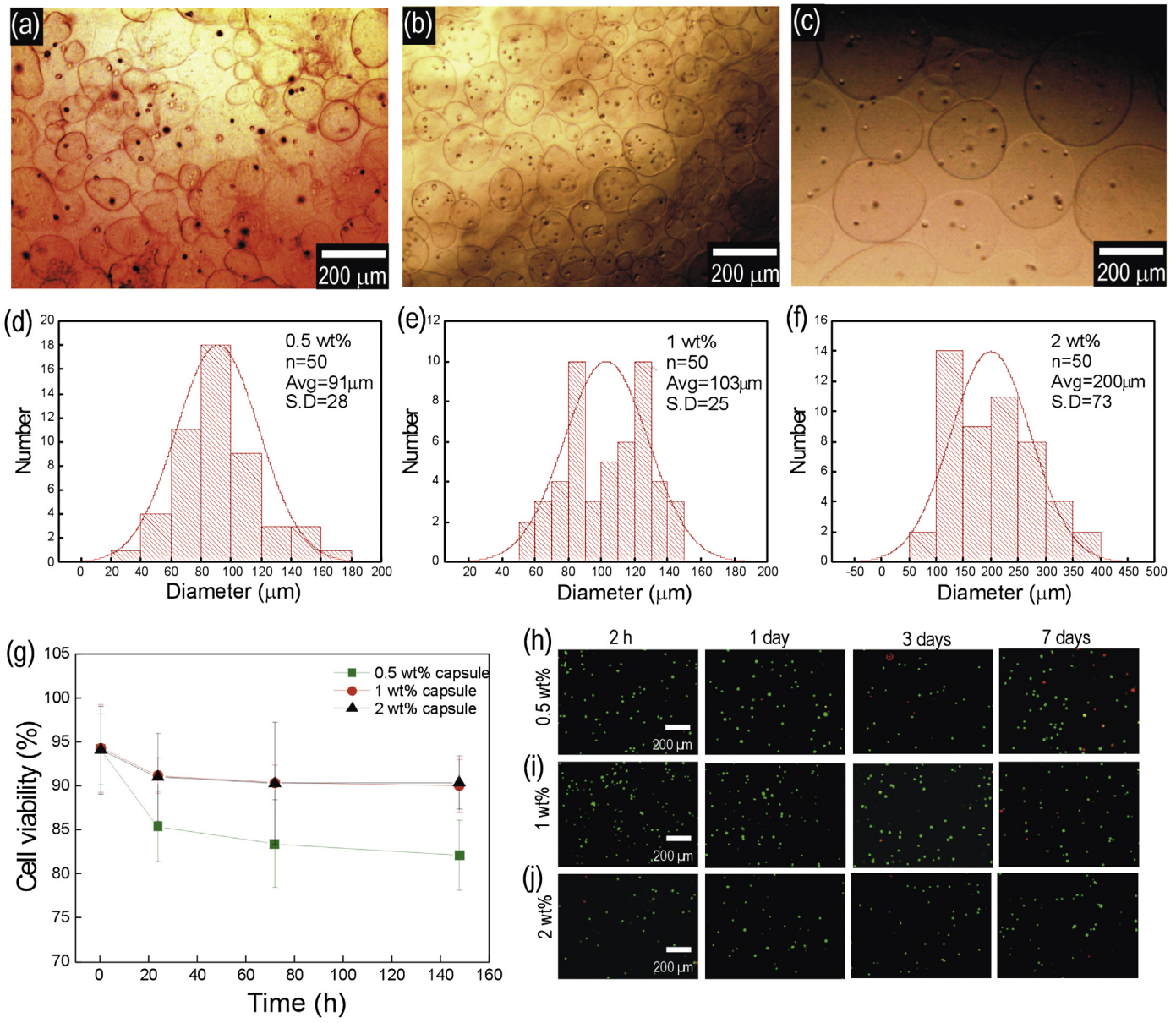

Fig. 3. Optical micrographs of fabricated cell-laden micro-beads for three alginate weight fractions [(a) 0.5 wt%, (b) 1 wt%, and (c) 2 wt%] and cells (2.2×10^5 mL^{-1}). (d–f) Size distributions and average diameters of fabricated cell-laden micro-beads. (g) Viability of cells embedded in micro-beads, fabricated using three alginate weight fractions. (h–j) Fluorescence images of live (green) and dead (red) cells after culture for 2 h and 1, 3, and 7 days. (For interpretation of the references to color in this figure legend, the reader is referred to the web version of the article.)

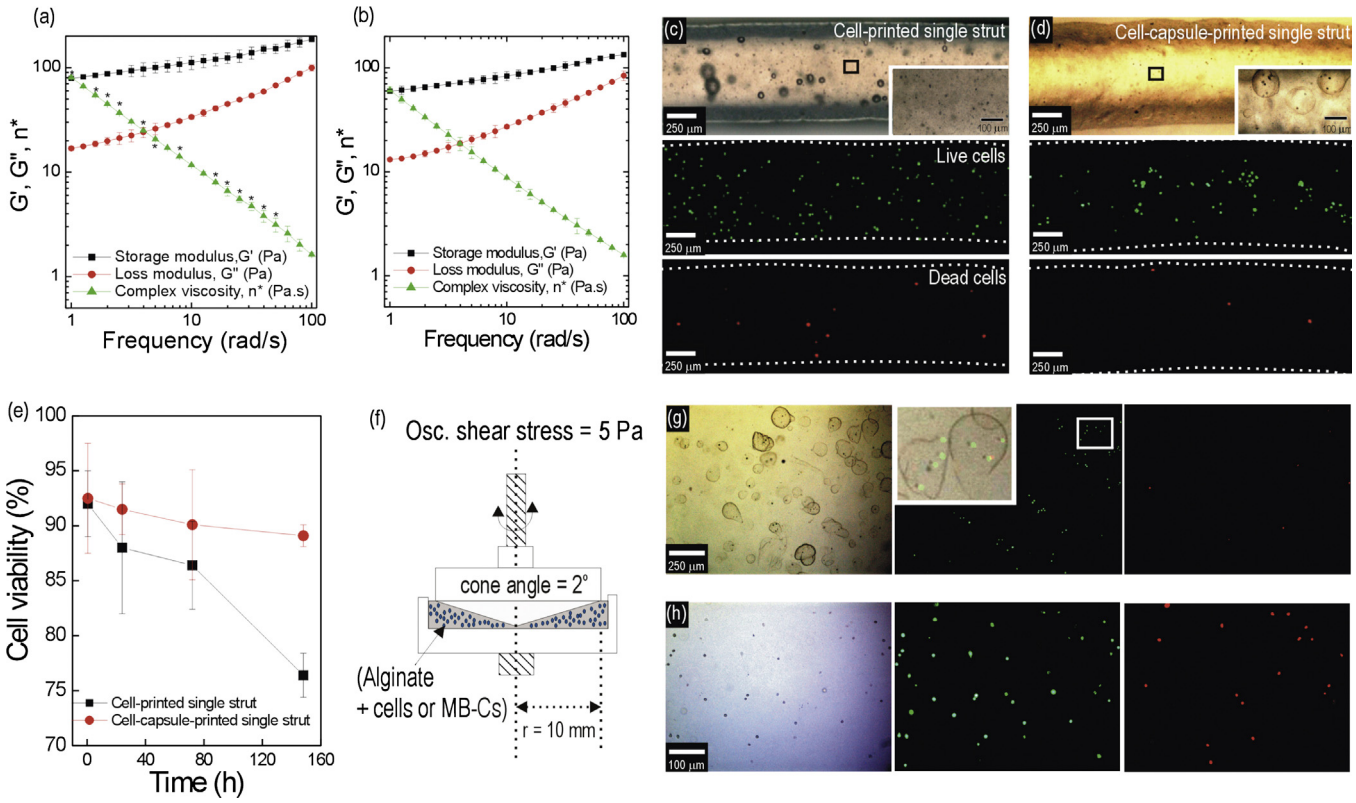

Fig. 4. Rheological results for (a) cell- and (b) MB-C-embedded alginate solutions (3.5 wt% alginate solution and 1.2×10^5 cells mL^{-1}). Optical and fluorescence images of a single strut for (c) pure cell-dispensed strut and (d) MB-C-dispensed strut. Inset images show the surface of the strut. (e) The viability of cells embedded in single strut for various culture periods. (f) Schematic of the application of oscillatory shear stress (5 Pa) on cell- and MB-Cs in alginate solution (3.5 wt%) with an identical cell density (1.2×10^5 mL^{-1}). After application of shear stress (5 Pa) for 10 min, optical and fluorescence images of live and dead (g) MB-Cs and (h) pure cells were obtained.

micro-beads, whose size differed due to the different viscosities of the spraying solution, irrespective of the pressure used (120 kPa). Mean micro-bead diameter increased, as the weight fraction of the alginate solution in the mixture increased, from 91 (0.5 wt% alginate) to 200 μm (2 wt% alginate) (Fig. 3(d)–(f)). The circularity, which is defined as a value between 0 and 1 indicating how closely the bead shape looks like a circle, of the fabricated beads (0.5, 1, and 2 wt% of alginate) was 0.76 ± 0.12, 0.87 ± 0.10, and 0.9 ± 0.12, respectively. The circularity was analysed for at least 50 beads.

We used the Image-J software to assess the viability of the fabricated MB-Cs. Fig. 3(g) shows the cell viability for MB-Cs fabricated using three different alginate weight fractions. Fig. 3(h)–(j) shows live (green) and dead (red) cells for the cell-laden beads fabricated with 0.5, 1, and 2 wt% alginate after culture for 2 h and 1, 3, and 7 days. As shown in Fig. 3(g), the viability of the cells in micro-beads fabricated with the 0.5 wt% alginate were significantly lower than those of other weight fractions (1 and 2 wt% alginate) from 1 to 7 days in culture. This may be due to use of calcium chloride

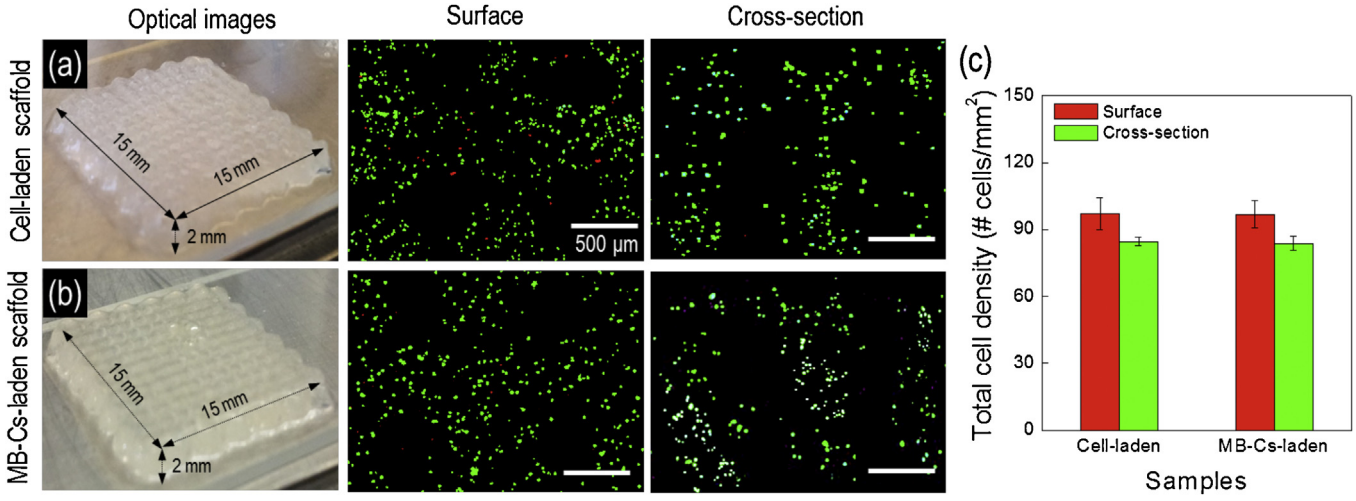

Fig. 5. Optical image of the scaffolds and fluorescence images of the surface and cross-sectional area of the scaffolds showing live (green) and dead (red) cells on (a) cell-laden scaffold and (b) MB-Cs-laden scaffold. (c) Comparison of cell density for surface and cross-section regions of the scaffolds. (For interpretation of the references to color in this figure legend, the reader is referred to the web version of the article.)

solution during bead fabrication. The shell obtained using the low alginate weight-fraction may have been too thin, so that the cross-linking agent may have diffused into the inner region of the beads, resulting in greater cell damage than those fabricated using higher alginate weight fractions (1 and 2 wt%). Additionally, when the alginate weight fraction was >1 wt%, cell viability was independent of alginate weight fraction. However, because use of cell-embedded micro-beads of an excessive size reduces the efficiency of nutrient and waste diffusion (Tan & Takeuchi, 2007), we used 1 wt% alginate to fabricate micro-sized beads.

3.2. Rheological properties of the cell-laden solution

To evaluate the effect of micro-beads on the rheological properties of the hydrogel solution, we measured the complex viscosity (n^*), storage (G'), and loss modulus (G'') for cell-laden alginate solution (Fig. 4(a)) and MB-Cs-laden alginate solution (Fig. 4(b)). The complex viscosity and storage modulus of the MB-C-containing solution were slightly lower than the pure cell-embedded alginate solution. Thus the MB-C solution may experience lower shear stress during the micro-syringe process than the cell-laden

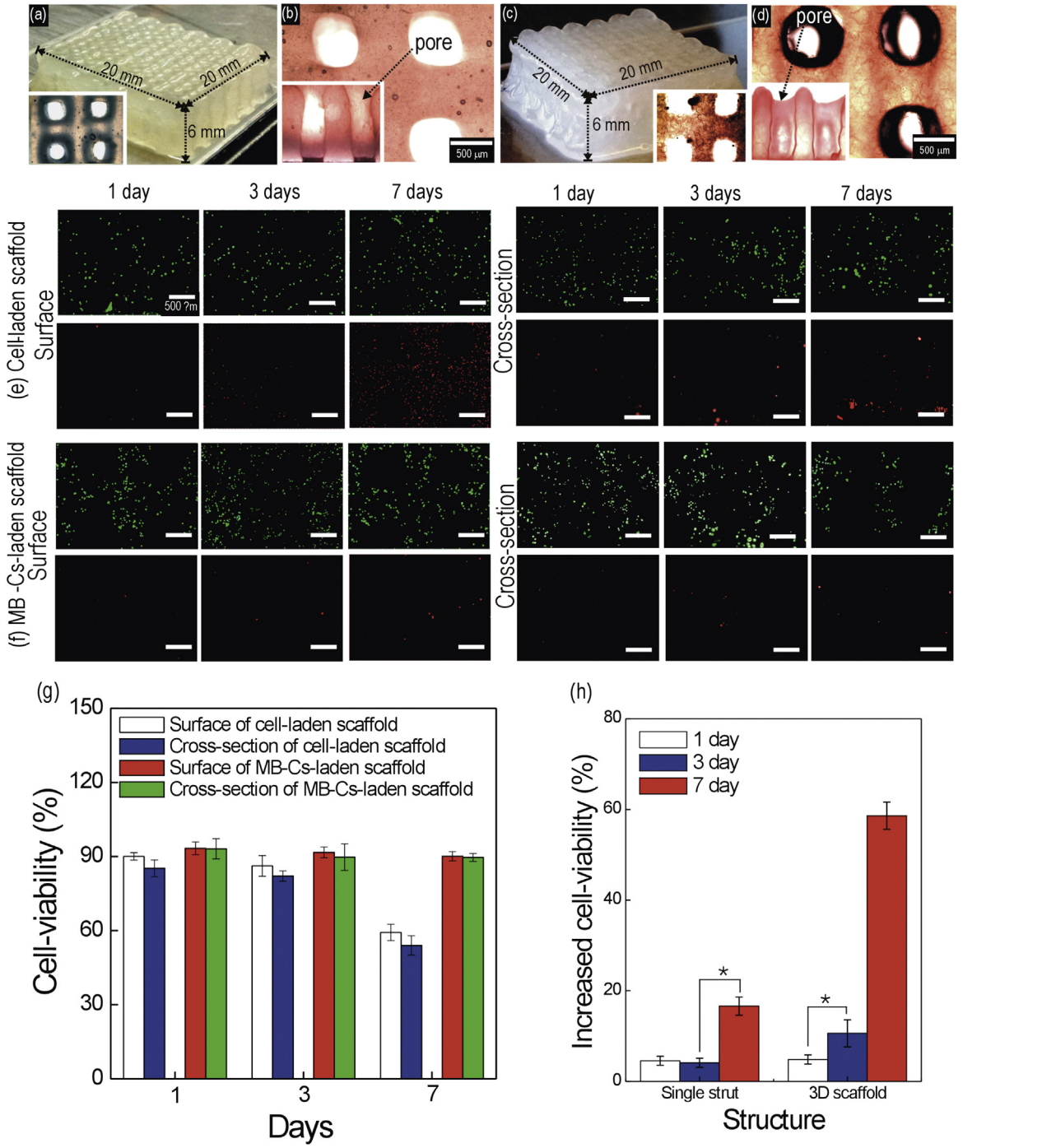

Fig. 6. Optical images of macroscopic 3D-alginate scaffolds embedded with (a) cells and (b) MB-Cs. Inset images show the fabricated pores. Optical and fluorescence images of (c) cell- and (d) MB-Cs-laden scaffolds, describing pore structure and live and dead cells after 7 days in culture. Inset images show the cross-section of the scaffold, indicating that the pores were well-connected, resembling a channel. (e) Cell viability of the 3D scaffolds. (f) Relative cell viabilities, normalised to those of a normally fabricated cell-laden singe strut and 3D scaffold, of single-alginate-strut and 3D-alginate scaffolds laden with MB-Cs. $^*p < 0.05$.

solution. The oscillatory shear stress at 10 rad s^{-1} was 2.2 Pa for the pure cell-laden alginate solution and 1.9 Pa for the MB-C solution.

3.3. Cell-viability of cell-laden struts supplemented with and without micro-beads

Using the MB-Cs in alginate solution, we fabricated a single strut and determined the effects of the micro-syringing process on cell viability. Fig. 4(c) and (d) shows optical and fluorescence images of cell- and MB-C-laden struts (live cells are green and dead cells are red). Both cells and MB-Cs were well-distributed throughout the alginate strut. Fig. 4(e) shows cell viability after 2 h and 1, 3, and 7 days. After 2 h, the cell viabilities were similar, but with increasing culture time, the mean viability of the simply dispensed cells decreased considerably, from 92% at 2 h to 76% at 7 days, while the viability of cells shielded within micro-beads was not markedly different between the initial state (93%) and 7 days (90%). Thus the MB-C-laden process enhances cell survival compared to the pure cell-dispensing process. This may be because the micro-beads not only protect against external shear and normal stress during extrusion from the micro-syringe, but also shield the cells from the cross-linking agent, calcium chloride, during the first and second cross-linking processes. To validate the shielding effect of the micro-beads against shear stress, we conducted a stress endurance test. Fig. 4(f) shows a schematic of the cone-and-plate geometry (cone angle = 2°, radius = 10 mm, and distance between cone and plate = 108 μm) in which alginate solution (3.5 wt%; 1.2×10^5 cells mL^{-1}) was injected between the cone and plate and a constant oscillatory shear stress (5 Pa) was applied over 10 min. The cell viability was then determined. Fig. 4(g) and (h) shows fluorescence images of the cell- and pure cell-laden micro-bead solutions. The viability of the micro-bead shielded cells was 91.5 ± 5.2%, compared to 72.9 ± 4.8% of the pure cells. As expected, the micro-beads protected the cells against shear stress. Generally, cell damage, *CD* (%), can be described by the power-law function to the applied wall shear stress and exposure time (t), $CD(\%) = C\tau_w^a t^b$, where C, a, and b are material constants (Grigioni et al., 2004; Li, Tian, & Chen, 2009). Based on this relation, the applied shear stress (τ_w) on the solution containing cell-beads was not critically transferred to the cells during the shearing process, which cannot cause serious damage to the cells.

3.4. In vitro cellular activities of cell-laden scaffolds

Homogeneous cell density is a significant factor for effective tissue regeneration using a scaffold because it can prominently influence cellular responses (proliferation and distribution of cells in the scaffold). To observe cell density, live and dead cells were analysed 12 h after fabrication. Fig. 5(a) and (b) shows optical and fluorescent images of the cell-laden and MB-Cs laded scaffolds, respectively. In the images, live cells are green and dead cells are red. Using the fluorescence images, cell density was measured with the total number of cells per mm^2. Fig. 5(c) shows the comparison of cell density for the cell-laden and MB-Cs laden scaffolds. The cell density between the scaffolds was similar, but the cell-density in the surface was slightly high as compared with that in the cross-section.

Generally, scaffold pore structure impacts cellular activities, because it provides a path for cell migration and proliferation as well as a transportation path for nutrients and waste (Murphy, Haugh, & O'Brien, 2010; Brien, Harley, Yannas, & Gibson, 2005). Therefore, fabrication of 3D macroscopic porous cell-laden hydrogel scaffolds is important. Several methods of preparing porous cell-laden structures have been proposed. We recently proposed a micro-syringe process, supplemented by an aerosol cross-linking method (Ahn, Lee, Bonassar, et al., 2012; Ahn, Lee, Puetzer, Bonassar, & Kim, 2012). Using this process, we obtained 3D porous cell-laden alginate scaffolds (Ahn, Lee, Bonassar, et al., 2012; Ahn, Lee, Puetzer, et al., 2012). Using the aerosol process, we attempted to fabricate hydrogel scaffolds embedded with MB-Cs. Fig. 6(a),(b) and (c),(d) shows micrographs of 20 mm × 20 mm × 6 mm 3D porous alginate hydrogel scaffolds containing pure cells and MB-Cs, respectively, indicating that the 3D pore structures were maintained, including the designed pores and channels extending uninterrupted from top to bottom. The scaffold shapes were prepared and the designed pore size (350–470 μm) was maintained during the process. As shown in the images, cells and MB-Cs were well-embedded in the pore structures. Fig. 6(e) and (f) shows surface and cross-sectional live-dead images of the scaffolds at 1, 3, and 7 days. Cell viability within the MB-C-laden alginate scaffold at 7 days was meaningfully higher than that of the pure cell-laden scaffold (Fig. 6(g)). This is likely due to shielding of the cells by the micro-beads during the cross-linking process and protection against external stresses during the micro-syringe process. Fig. 6(h) shows a comparison of the relative increase (%) in

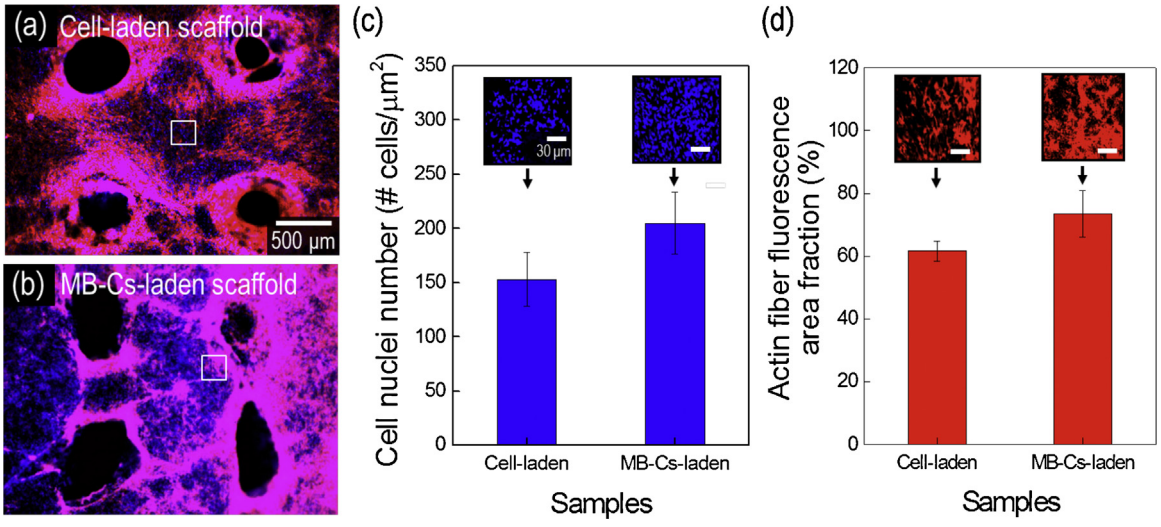

Fig. 7. Fluorescence images showing nuclei (blue) and F-actin (red) for the (a) cell-laden scaffold and (b) MB-Cs-laden scaffold after 62 days in culture. (c) Cell density (cells/μm^2) and (d) F-actin area (%) of the scaffolds. (For interpretation of the references to color in this figure legend, the reader is referred to the web version of the article.)

cell-viability, [(cell-viability of MB-Cs in the scaffold) − (cell-viability of the normal cell-dispensed scaffold)]/(cell-viability of the normal cell-dispensed scaffold) × 100, during culture over several days, of a single strut and a scaffold. The increasing trend in cell viability for both a single strut and a 3D scaffold was similar, but the value of the 3D scaffold at 7 days was markedly higher, indicating that the cell-laden micro-bead process was more effective in the 3D complex porous structure.

Fig. 7(a) and (b) shows fluorescence images showing the stained nuclei (blue) and F-actin (red) after 62 days culture for cell-laden scaffold and MB-Cs-laden scaffold, respectively. As shown in the images, the cells with the ECM proliferated well, and, in particular, for MB-Cs-laden scaffold, the cells grew more effectively as compared to cell-laden scaffold (Fig. 7(c) and (d)).

4. Conclusions

In summary, we propose here a novel cell-encapsulation method consisting of alginate struts with MB-Cs. Fabrication was conducted using a three-axis robot system and an aerosol-spraying method. By adjusting the micro-bead fabrication process, we successfully obtained reasonable cell viability (>90% after 7 days in culture) throughout the scaffold. Based on this realistic macroscopic 3D cell-laden hydrogel scaffold with a highly porous structure (homogeneous pore size and 100% pore interconnectivity), we believe that this fabrication method will be useful in various tissue regeneration applications.

Acknowledgments

G.H. Kim is grateful to Prof. L. Bonassar for his permission for using various facilities in his laboratory of the Cornell University. This research was financially supported by the National Research Foundation of Korea grant funded by the Ministry of Education, Science, and Technology (MEST) (Grant No. NRF-2012R1A2A2A01017435) and also was partially supported by a grant of the Korean Health Technology R&D Project, Ministry of Health & Welfare, Republic of Korea (Grant No. A120942).

References

Ahn, S. H., Lee, H. J., Bonassar, L. J., & Kim, G. H. (2012). Cells (MC3T3-E1)-laden alginate scaffolds fabricated by a modified solid-freeform fabrication process supplemented with an aerosol spraying. *Biomacromolecules*, *13*, 2997–3003.

Ahn, S. H., Lee, H. J., Puetzer, J., Bonassar, L. J., & Kim, G. H. (2012). Fabrication of cell-laden three-dimensional alginate-scaffolds with an aerosol cross-linking process. *Journal of Materials Chemistry*, *22*, 18735–18740.

Cohen, D. L., Lo, W., Tsavaris, A., Peng, D., Lipson, H., & Bonassar, L. J. (2011). Increased mixing improves hydrogel homogeneity and quality of three-dimensional printed constructs. *Tissue Engineering Part C: Methods*, *17*, 239–248.

Cohen, D. L., Malone, E., Lipson, H., & Bonassar, L. J. (2006). Direct freeform fabrication of seeded hydrogels in arbitrary geometries. *Tissue Engineering*, *12*, 1325–1335.

Fedorovich, N. E., Schuurman, W., Wijnberg, H. M., Prins, H.-J., van Weeren, P. R., Malda, J., et al. (2012). Biofabrication of osteochondral tissue equivalents by printing topologically defined, cell-laden hydrogel scaffolds. *Tissue Engineering Part C: Methods*, *18*, 33–44.

Fukuda, J., & Nakazawa, K. (2005). Orderly arrangement of hepatocyte spheroids on a microfabricated chip. *Tissue Engineering*, *11*, 1254–1262.

Gaetani, R., Doevendans, P. A., Metza, C. H. G., Alblas, J., Messina, E., Giacomello, A., et al. (2012). Cardiac tissue engineering using tissue printing technology and human cardiac progenitor cells. *Biomaterials*, *33*, 1782–1790.

Grigioni, M., Daniele, C., Morbiducci, U., D'Avenio, G., Benedetto, G. D., & Barbaro, V. (2004). The power-law mathematical model for blood damage prediction: Analytical developments and physical inconsistencies. *Artificial Organs*, *28*, 467–475.

Li, M. G., Tian, X. Y., & Chen, X. B. (2009). A brief review of dispensing-based rapid prototyping techniques in tissue scaffold fabrication: Role of modeling on scaffold properties prediction. *Biofabrication*, *1*, 032001.

Lum, Z. P., Krestow, M., Tai, I. T., Vacek, I., & Sun, A. M. (1992). Xenografts of rat islets into diabetic mice: An evaluation of new smaller capsules. *Transplantation*, *53*, 1180–1183.

Matsunaga, Y. T., Morimoto, Y., & Takeuchi, S. (2011). Molding cell beads for rapid construction of macroscopic 3D tissue architecture. *Advanced Materials*, *23*, 90–94.

Mironov, V., Kasyanov, V., & Markwald, R. R. (2011). Organ printing: From bioprinter to organ biofabrication line. *Current Opinion in Biotechnology*, *22*, 667–673.

Mironov, V., Visconti, R. P., Kasyanov, V., Forgacs, G., Drake, C. J., & Markwald, R. R. (2009). Organ printing: Tissue spheroids as building blocks. *Biomaterials*, *30*, 2164–2174.

Murphy, C. M., Haugh, M. G., & O'Brien, F. J. (2010). The effect of mean pore size on cell attachment, proliferation and migration in collagen–glycosaminoglycan scaffolds for bone tissue engineering. *Biomaterials*, *31*, 461–466.

O'Brien, F. J., Harley, B. A., Yannas, I. V., & Gibson, L. J. (2005). The effect of pore size on cell adhesion in collagen-GAG scaffolds. *Biomaterials*, *26*, 433–441.

Okushima, S., Nisisako, T., Torii, T., & Higuchi, T. (2004). Controlled production of monodisperse double emulsions by two-step droplet breakup in microfluidic devices. *Langmuir*, *20*, 9905–9908.

Ovsianikov, A., Deiwick, A., van Vlierberghe, S., Dubruel, P., Moller, L., Drager, G., et al. (2010). Laser fabrication of three-dimensional CAD scaffolds from photosensitive gelatin for applications in tissue engineering. *Biomacromolecules*, *12*, 851–858.

Park, Y. G., Iwata, H., & Ikada, Y. (1998). Microencapsulation of islets and model beads with a thin alginate–Ba^{2+} gel layer using centrifugation. *Polymers Advanced Technologies*, *9*, 734–739.

Pirlo, R. K., Wu, P., Liu, J., & Ringeisen, B. (2012). PLGA/hydrogel biopapers as a stackable substrate for printing HUVEC networks via BioLP™. *Biotechnology and Bioengineering*, *109*, 262–273.

Takeuchi, S., Garstecki, P., Weibel, D. B., & Whitesides, G. M. (2005). An axisymmetric flow-focusing microfluidic device. *Advanced Materials*, *17*, 1067–1072.

Tan, W.-H., & Takeuchi, S. (2007). Monodisperse alginate hydrogel microbeads for cell encapsulation. *Advanced Materials*, *19*, 2696–2701.

Yamato, M., & Okano, T. (2004). Cell sheet engineering. *Materials Today*, *7*, 42–47.